14th International Conference on CFD in
Oil & Gas, Metallurgical and Process Industries
SINTEF, Trondheim, Norway, October 12–14, 2020

SINTEF
**PROCEEDINGS**
6

# Proceedings from the 14th International Conference on CFD in Oil & Gas, Metallurgical and Process Industries

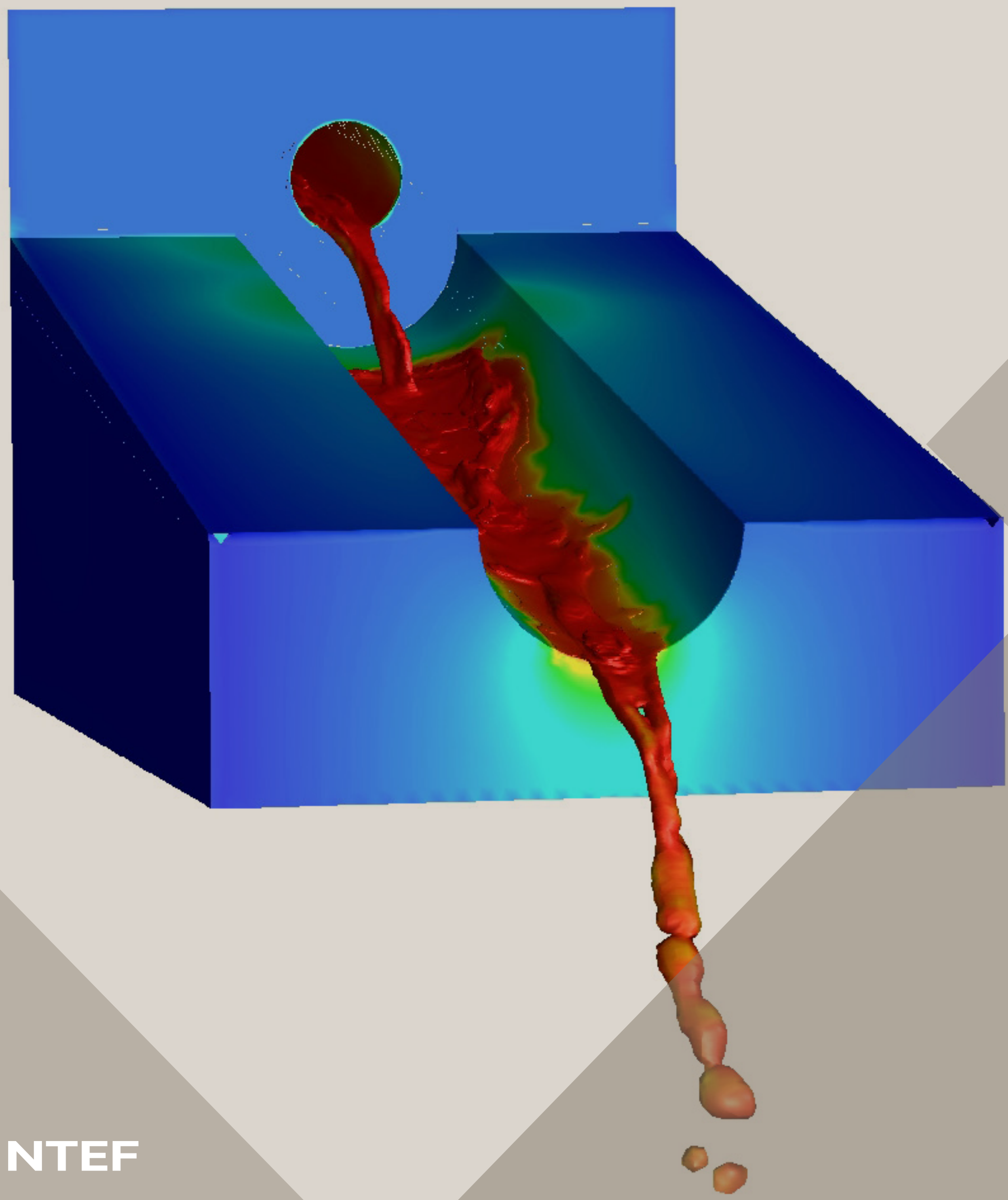

SINTEF

SINTEF Proceedings

Editors:
Jan Erik Olsen, Jan Hendrik Cloete and Stein Tore Johansen

# Proceedings from the 14th International Conference on CFD in Oil & Gas, Metallurgical and Process Industries

SINTEF, Trondheim, Norway
October 12–14, 2020

SINTEF Academic Press

SINTEF Proceedings 6
Editors: Jan Erik Olsen, Jan Hendrik Cloete and Stein Tore Johansen

Proceedings from the 14th International Conference on CFD in Oil & Gas, Metallurgical and Process Industries, SINTEF, Trondheim, Norway, October 12–14, 2020

Keywords:
CFD, fluid dynamics, modelling

Cover illustration: Tapping of metal by Jan Erik Olsen

ISSN 2387-4295 (online)
ISBN 978-82-536-1684-1 (pdf)



SINTEF Academic Press
Address: Børrestuveien 3
PO Box 124 Blindern
N-0314 OSLO
Tel: +47 40 00 51 00

www.sintef.no/community
www.sintefbok.no

SINTEF Proceedings
SINTEF Proceedings is a serial publication for peer-reviewed conference proceedings on a variety of scientific topics.
The processes of peer-reviewing of papers published in SINTEF Proceedings are administered by the conference organizers and proceedings editors. Detailed procedures will vary according to custom and practice in each scientific community.

# CFD modelling of an accidental release of a methane and hydrogen sulfide mixture in an offshore platform

**Gianmario Ledda, Alberto Moscatello, Anna Chiara Uggenti, Raffaella Gerboni, Andrea Carpignano**

Department of Energy, Politecnico di Torino, corso Duca degli Abruzzi, 24, 10141 Torino, Italy
E-mail: gianmario.ledda@polito.it
E-mail: alberto.moscatello@polito.it
E-mail: anna.uggenti@polito.it
E-mail: raffaella.gerboni@polito.it
E-mail: andrea.carpignano@polito.it

## ABSTRACT

Oil & Gas plants are complex systems involving dangerous substances, potential origin of severe accidental scenarios. Therefore, according to Directive 2013/30/EU, a Risk Assessment (RA) is mandatory. A fundamental step of the RA is the accident simulation to evaluate the damage area involved by each accidental scenario.

One of the main issues of natural gas extraction platforms is the presence of traces of hydrogen sulfide ($H_2S$) in the extracted mixture. When the $H_2S$ is present in the natural gas, the mixture is called sour gas. The presence of $H_2S$ is of great interest since it is flammable, colorless and highly toxic, therefore, highly dangerous to people. Several literature studies demonstrate that it is common to have mixtures with 2 % to 20 % by weight $H_2S$ in Oil & Gas facilities reservoirs, underlying how this problem is of common interest.

In this work a highly pressurized (50 bar) accidental release of a methane-hydrogen sulfide mixture (95 % $CH_4$ – 5 % $H_2S$) in the production deck of an Oil & Gas platform is treated. Due to the complexity of the geometry and the need to accurately define the dangerous areas, the Computational Fluid Dynamics (CFD) is chosen to simulate the event instead of the commonest empirical models.

In particular, the multi-scale and multi-physics nature of the involved phenomena represent a real challenge for the CFD simulation implementation. In fact, as the gas is released from high pressures (10 bars or more) into the ambient, a highly under-expanded jet develops: a supersonic velocity is reached (Ma >> 1) near the release point where a Mach disk appears and produces very strong discontinuities in the flow-field variables (pressure, velocity, density, temperature, etc.). As the gas slows down, a subsonic dispersion follows in the main portion of the deck, where the velocity gradients rapidly decrease, and the buoyancy effects become dominant.

This work proposes a CFD two-steps approach implemented on ANSYS Fluent, called SBAM (Source-Box Accident Model) to simulate the accident in order to account for the different physics involved, in order to evaluate the damage areas affected.

**Keywords:** accidental gas release, risk, safety, CFD fluid dynamics, ANSYS Fluent, Oil & Gas, offshore facilities, hydrogen sulfide

## NOMENCLATURE

*Greek Symbols*

$\rho$ Mass density, [kg/m$^3$].

*Latin Symbols*

d Diameter, [m].
p Pressure, [bar].
$\vec{v}$ Velocity, [m/s].
Ma Mach number, [-].
$y^+$ Dimensionless wall distance, [-].
$Y_i$ Local mass fraction of *i*th species, [-].
$R_i$ Net rate of production of *i*th species, [kg/m$^3$/s].
$S_i$ Source term of *i*th species, [kg/m$^3$/s].
$\vec{J_i}$ Diffusion flux of *i*th species, [kg/m$^2$/s].
t time, [s].

## INTRODUCTION

Nowadays, the Risk Assessment implementation tools are being continuously improved for risk-relevant industrial applications that involve hazardous substances, e.g. Oil & Gas facilities, chemical plants, nuclear installations (Patè-Cornell, 1993 and Necci et al., 2019). Quantitative Risk Assessment (QRA) is fundamental and mandatory according to European guidelines to guarantee the industrial plant sustainability (Casal, 2007 and Vinnem, 2019). This procedure requires the analysis of numerous accidental scenarios in order to perform an exhaustive consequence analysis. This work takes into account an Oil & Gas offshore platform offering an improvement in the accident simulations to enhance the sustainability of the consequences analysis process. The state-of-practice for onshore facilities involves the use of empirical models (e.g. Chen and Rodi, 1980, Davidson, 1967 and Zamejc, 2014) to estimate the damage areas associated to the accidental events, due to their fast response. Meanwhile, in the offshore applications,

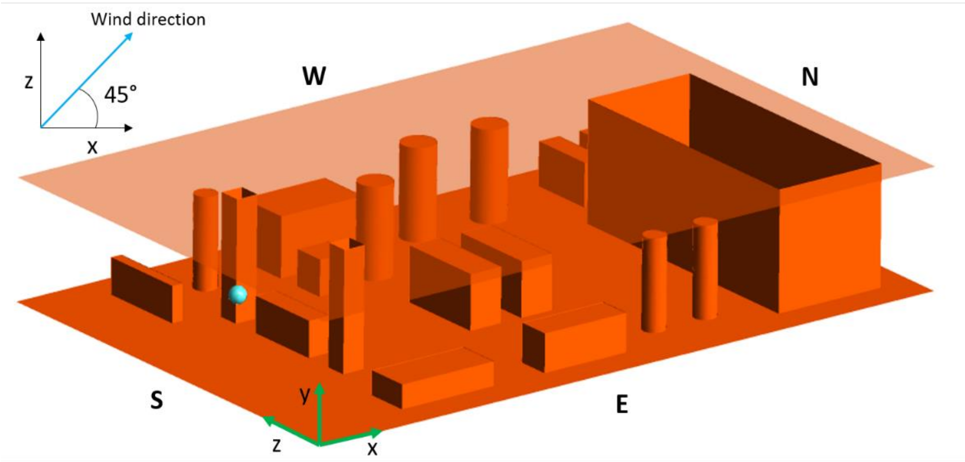


Figure 1: Production deck CAD, wind direction, release point (blue sphere).

characterized by complex geometries and congested environments, the empirical models lead to a large overestimation of the damage areas and to an oversizing of protections, which involve the growth of construction cost and a mechanical overload of the offshore structure. From the last considerations, the necessity to find another approach for consequences' estimation in complex structures arises. The SEADOG Lab Group of Politecnico di Torino, driven by this necessity, proposed a novel CFD method, called SBAM (Source Box Accident Model) aiming at guaranteeing a suitable cost-accuracy trade-off for the simulation of accidental releases of a pressurized gas in congested industrial environments. The SBAM approach splits the phenomenon in two different CFD simulations, realized in ANSYS Fluent, in order to properly treat its multiscale and multi physics nature and to speed-up the simulation for obtaining a computational time compatible with the QRA procedure (detailed description in section 3). Different authors have already proposed this two-steps method (Venetsanos et al., 2008, Choi et al., 2013, Liu et al., 2014 and Deng et al., (2018)), but they used a hybrid empirical-CFD approach to simulate the event, while here a full CFD method is proposed because the congested environment requires to model the first phase of the phenomenon in a reliable way .

This paper would not have been possible without the sponsorship of the Ministry of Economic Development's Directorate General for Safety – National Mining Office for Hydrocarbons and Georesources.

### Objective of the work

In this work, a high-pressure sour gas release in an offshore platform production deck is analysed. The SBAM approach is applied to a specific case study to obtain the damage distances useful for flammable and toxic maps of a QRA. The objective of this paper is to show how the method works considering a flammable and toxic gas mixture, its advantages and its flexibility to identify the damage areas consequent to an offshore accidental scenario.

## PROBLEM DESCRIPTION

### Sour gas in offshore environment

In the offshore extraction platform, the natural gas is mainly composed by methane with traces of other volatile hydrocarbons, carbon dioxide, nitrogen and hydrogen sulfide. The hydrogen sulfide ($H_2S$) is the major pollutant in natural gas and, when it is present, the natural gas is called sour gas. $H_2S$ is a colourless, flammable and highly toxic gas. Several Oil&Gas extraction facilities observe the presence of hydrogen sulfide in their reservoirs and many studies are performed on the amount of $H_2S$ in natural gas. As suggested by (Worden et al., 2003), in the North Sea the natural gas can contain up to the 2 vol% of $H_2S$; according to (Zempolich et al.,2002) and (Warner et al., 2007), the Kazakh gas fields of Kashagan and Tengiz can reach contents of 19 vol% and 16 vol% of $H_2S$ respectively; in the Sichuan Basin, the percentage of $H_2S$ in natural gas can vary between 10 vol% and 17 vol% as suggested by (Liu et al.,2010); with reference to (Mi et al., 2017) the natural gas extracted from Eastern Venezuela Basin contains the ~ 5 vol% of $H_2S$.
An accidental high-pressure release of sour gas can lead to several major hazards like explosions, fires or intoxication. Moreover, the presence of $H_2S$ can cause several damages to the process components due to its corrosive properties, increasing the failure rate due to leakages (Li et al., 2014). The effects of sour gas release can be dramatic for the people and the environment, as observed during the Lodgepole blowout accident in Alberta in 1982 (Layfon and Cederwall, 1987), up to now the biggest release of sour gas.

### Case study

The sour gas release in a production deck (shown in Fig. 1) analysed here is defined by a set of relevant parameters:

- Release conditions: $p_0 = 50\ bar, T_0 = 300\ K$
- Release hole diameter: $d_e = 3\ cm$
- Released gas mixture molar composition: $95\ mol\%\ CH_4 - 5\ mol\%\ H_2S$
- Wind velocity: $v = 6\ m/s$
- Wind direction: 0.5x + 0.5z (Fig. 1)
- Ambient temperature: $T_a = 300\ K$

- Release position x = 3 m, y= 2.5 m, z = 10 m and direction x (light blue sphere in Fig. 1);

The release pressure and hole diameter values (a circular hole is assumed) are chosen in agreement with (Vivalda et al., 2018) and are considered representative for Oil & Gas field. The selected wind intensity is typical of Italian platforms installed in the Adriatic Sea. The mixture molar composition is chosen according to the literature review exposed in section 2.1.

## METHODOLOGY

In this work, the SBAM method is applied and it is characterised by the splitting of the accidental release in two different simulations.
This necessity arises from the phenomenon multi-physics and multi-scaling nature. In fact, since the gas, in case of accident, is released at high pressure (10 bar or more), a highly under-expanded jet results (Franquet et al., 2015) with strong compressible effects, as the presence of a Mach disk. This phenomenon is confined in a very small portion of the domain, near the release point, where the flow is compressible (Ma>0.3) (Munson et al., 2009). At a certain distance from the release point, the gas flows, it reaches subsonic velocities (Ma<0.3) so that the flow can be assumed incompressible and a gas dispersion occurs in the remaining part of the domain, the biggest one.
Consequently, the splitting of the phenomenon into a supersonic-compressible discontinuous flow (the *release*) and an incompressible-subsonic smooth flow (the *dispersion*) results convenient for modelling purposes.
The SBAM method consists in simulating the *release* in a small domain, the Source-Box (SB), dimensioned to contain all the compressibility effects (see paragraph 3.1.1), and setting the right models to account for these effects and a suitable mesh to capture the discontinuities in the Mach disk region. The results of this *release* model are the profiles of velocity and mass fraction of the pollutant gas on the outer faces of the SB, representing the interface with the domain of the *dispersion* modelling (section 3.2.1); in the latter, the mesh can be rough as no complex fluid dynamic structures are expected.
As shown in the results, this approach permits to have a fast dispersion evaluation. Moreover, the same SB results can be used for many dispersion simulations just changing the release position and direction in the domain. This outcome is relevant especially from a QRA point of view, since this procedure requires the simulation of many scenarios in a relatively short time.

### Release simulation (Source-Box)

*Design and mesh*

The SB presents a cubic shape with dimensions defined to guarantee that all the compressibility effects are exhausted inside its domain. (Crist et al., 1966) suggest that the compressible effects become negligible when the distance from the release point is ten times the distance of the Mach disk ($X_m$). Several authors, as (Franquet et al, 2015), have conducted numerical and experimental studies to obtain a correlation to define the Mach disk position. (Franquet et al, 2015) suggest the following definition of $X_m$:

$$X_m = 0.645 \cdot d_e \cdot \sqrt{\frac{p_0}{p_{amb}}} \qquad (1)$$

where $p_{amb}$ is the ambient pressure. Then, according to (Crist et al., 1966), the SB side length ($L_{SB}$) is:

$$L_{SB} = 10 \cdot X_m \qquad (2)$$

Using the parameters presented in 2.2 the characteristic length of the SB of this case study is $L_{SB}$ = 1.38 m.
Another important feature of the SB is the presence of an obstacle in front of the release point, since it is likely to occur in industrial congested plants. In this case, a cylinder with diameter 30 cm is located at a distance of 45 cm from the release point.
An unstructured tetrahedral mesh is chosen as it better suits complex geometries and it is suggested for non-directional flows (ANSYS Fluent, 2018). A non-uniform mesh with a major refinement in the Mach disk region and near the cylindrical obstacle is created; to assure the solution independence from the chosen grid a convergence study is performed obtaining a ~9.5e4 elements mesh with an average size of computational cell of ~5e-3m and a refinement around the release hole with a cell of ~2e-3m. The Fluent inflation algorithm is used to model the boundary layer near the nozzle wall and the obstacle, the first cell height is chosen in order to obtain $y^+ < 5$ in the wall region (Munson et al., 2009).

*Source-Box simulation setup*

To model the highly under-expanded jet of $CH_4$-$H_2S$ mixture, a 3D steady-state simulation is set. This choice is made because the detection time of the safety detectors is longer than the transient time of the phenomenon: the dangerous substance cloud reaches the steady-state configuration before the gas detectors can detect the presence of the hazardous atmosphere. According to (Doroudi et al., 2015), a Pressure-Based Coupled Algorithm is selected (ANSYS Fluent, 2018). A pressure inlet of 50 bar, a $CH_4$ mole fraction equal to 0.95 and a $H_2S$ mole fraction equal to 0.05 are imposed at the nozzle inlet. A wall with no-slip condition is imposed on the nozzle external surface and the cylinder surface. A pressure outlet set at atmospheric pressure is imposed on all the external SB surfaces to reproduce the open environment around.
Due to the compressible nature of the flow, the temperature field must be evaluated by solving the energy equation in order to calculate the density. The SST k-ω turbulence model, validated for under-expanded jets by (Novembre et al., 2006) and (Liu et al., 2014) against the available experimental data (Eggins and Jackson, 1974), is selected for the purposes of this study. Moreover, since a y+ < 5 is obtained at the walls, the SST k-ω model guarantees a proper boundary layer evaluation. The viscous dissipation term is selected to describe the thermal energy due to viscous shear in the flow, which is relevant for high velocity compressible flows (ANSYS Fluent, 2018). To model the interaction

between different chemical species ($CH_4$-$H_2S$-Air) the "Species Transport" model is used in order to solve a transport equation without chemical reactions. The "constant dilute approximation" provided by ANSYS Fluent is considered by setting a value ~2e-5 $m^2/s$ in order to take into account the diffusion of the chemical species in the air. The same assumption is made for the dispersion simulation as well.

The local mass fraction of each species ($Y_i$) is predicted using the transport equation in the following form:

$$\frac{\partial}{\partial t}(\rho Y_i) + \nabla \cdot (\rho \vec{v} Y_i) = -\nabla \cdot \bar{J}_i + R_i + S_i \qquad (3)$$

where $R_i$ is the net rate of production of species and $S_i$ is a source term.

A pseudo-transient model is used in order to relax the solution. This option is a form of implicit under-relaxation that guarantees a better convergence of the solution.

## Dispersion simulation

*Design and mesh*

The simulation domain is shown in Fig. 1. For the dispersion simulation, a simplified CAD of the production deck is considered; in order to simplify the geometry of the study the deck minor equipment is neglected. It should be noticed that the roof and the floor of the deck are plated walls, typical of gas extraction platforms in order to limit the hazardous areas involved in the accidental scenario if a leakage occurs.

Due to the complexity of the geometry, an unstructured tetrahedral mesh is generated. This choice is also due to the fact that the use of structured meshes for the discretization of complex geometries with curves can require high time-consuming processes and low quality meshes (e.g. high skewness, etc.). Coherently, (ANSYS Fluent, 2018) suggests that an unstructured mesh is more efficient in the distribution of the elements, especially when curved objects are present. Finally, also for this simulation a grid convergence study is performed, and the resulting mesh consists of ~3e6 elements with an average computational cell size of ~0.5 m and a face refinement on the obstacles of ~0.15 m and on the SB about of ~1 cm.

*Dispersion simulation setup*

As the release simulation, also the dispersion simulation is performed in steady-state since the final purpose is the estimation of the cloud dimensions at steady-state conditions because of the flammability and toxicity of the released mixture. In addition, in view of a CFD-QRA integration, a transient simulation will lead to high computational cost.

To describe the assumed boundary conditions, Fig. 1 can be taken as a reference. On the South and East side of the platform, a *velocity inlet* is imposed to reproduce the wind velocity of 6 m/s and the direction explained in the case study explanation in 2.2. On the North and West side a *pressure outlet* is used to impose an atmospheric pressure. In fact, as the deck lateral faces are open, the gas cloud can escape the domain due to its dispersion and the wind effect. The deck floor, the ceiling and all the obstacles inside the deck are modelled as *walls with no-slip* conditions. The results of the SB simulation are used as boundary conditions of the dispersion simulation to simulate the release; for this purpose, a box with the same dimensions of the SB is created in the domain in the release position. On its faces the $CH_4$ m.f. (mass fraction), $H_2S$ m.f. and velocity profiles are imposed (Fig. 3, Fig. 4, Fig. 5).

The turbulence model employed in the calculation is an SST k-ω as it has been validated for subsonic dispersions of methane in a room by (Li et al., 2016), against the experimental data obtained by (Ivings et al., 2010).

The choice of a RANS model can be justified by considering that a fast evaluation is desirable and, for our purposes (i.e. the evaluation of damage areas and volumes), an average distribution of the variables of interest (such as the $CH_4$ and $H_2S$ mass fraction, the velocity, etc.) is sufficient.

For this simulation as well as for the SB one, the species transport model (Eq. 3) is used to model the $CH_4$ – $H_2S$ - air interaction; no chemical reaction is considered in both release and dispersion simulations, therefore no $CO_2$ and water vapor will form during the event.

Particular attention is paid to the relaxation factors, as the species interaction causes oscillations in the residuals in most of the cases. Therefore, a fine tuning of the species relaxation factors is necessary. For example, at first, very low values of $CH_4$ and $H_2S$ equations relaxation factors are used, e.g. 0.5; once the residuals began to be smooth, these values are incremented to 0.8 until the simulation converges. The convergence is evaluated looking at some significant indicators like the average velocity at the outlet, the mass integral of $CH_4$ and $H_2S$: when they reach a plateau, the simulation is stopped.

# RESULTS

## Release phase results

A first discussion of the results is made in order to check their physical consistency. The high release pressure (50 bar) causes the formation of a highly under-expanded jet, which structure is very well known and studied in the past (Franquet et al., 2015). Therefore, it is important to check if the fluid-dynamic structure resembles the theoretical one. For this purpose, Fig. 2, which shows the midplane section of the SB, can be considered.

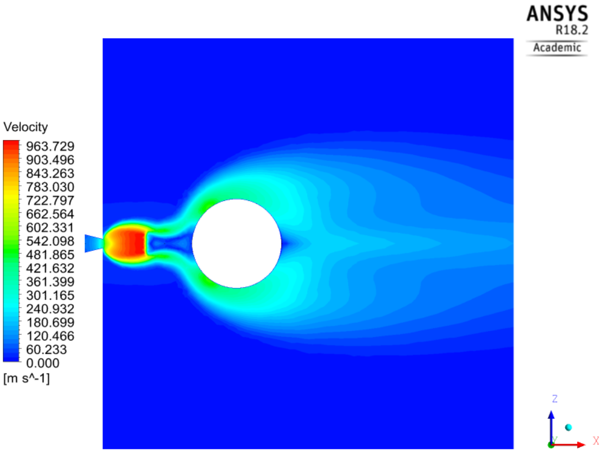


Figure 2: Velocity field in the SB midplane

As expected, the jet presents the typical fluid-dynamic structure: a supersonic core appears near the release point and a normal shock (Mach disk) divides the supersonic core from a subsonic region. Furthermore, the jet obstacle interaction reproduces a strong Coanda effect, as the fluid tends to follow the convex cylinder surface. To assess the accuracy of the solution in the most critical region, i.e. around the Mach disk characterized by strong discontinuities in the flow filed, the distance of the disk is compared to that obtained by using (Eq.1).
In Table 1, the values obtained by CFD and theory are detailed.

**Table 1: Mach disk location**

| $X_m$ (Eq. 1) [m] | $X_m$ (CFD) [m] | Relative error [%] |
|---|---|---|
| 0.1368 | 0.1300 | 4.97 |

The accuracy of the Mach disk location obtained by CFD can be considered satisfactory and physically consistent as the relative error with respect to the theoretical value is small enough.
At this point, it is important to analyze the important results for the SBAM method; in Fig. 3, Fig. 4 and Fig. 5 the velocity, $CH_4$ m.f. and $H_2S$ m.f. contours on the external SB surfaces are shown respectively.

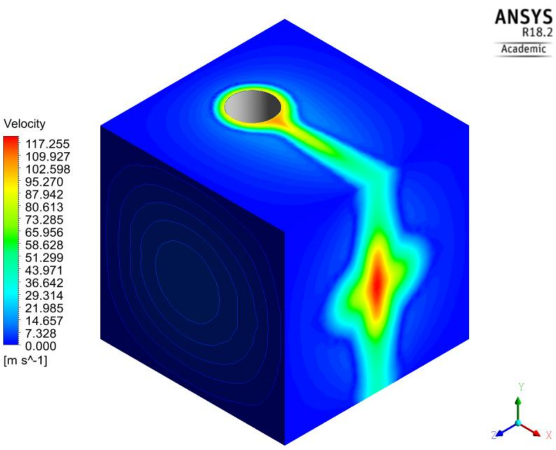


Figure 3: Velocity contours of SB outer surfaces

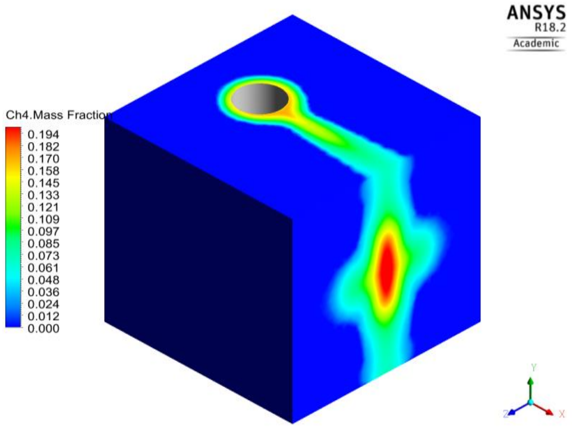


Figure 4: $CH_4$ mass fraction contours of SB outer surfaces

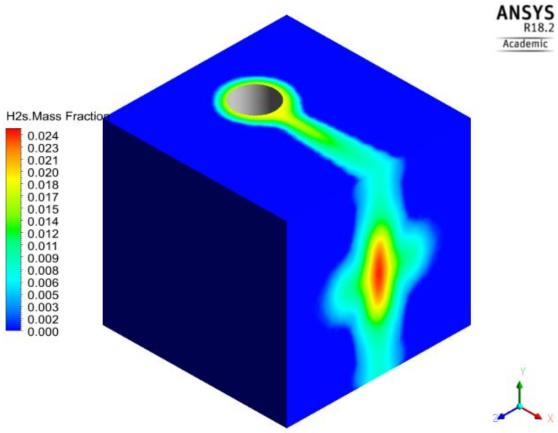


Figure 5: $H_2S$ mass fraction contours of SB outer surfaces

These profiles are crucial, since they represent the input boundary conditions of the dispersion simulation. It can be appreciated that the flow has enough inertia to close after the cylinder. The jet opening is more pronounced in the midplane of the SB, the release plane, since the momentum of the fluid is higher than in the other SB sections. The temperature field analysis is neglected because the released gas and the ambient are at the same temperature. Near the release point, it is possible to observe the temperature of the jet decreasing in correspondence of the Mach disk, but the fast mixing between the jet and the surrounding ambient air maintains the $CH_4$-$H_2S$ mixture near the ambient temperature. For this reason, also in the dispersion simulation the temperature field is not discussed.

### Dispersion phase results

Before discussing the results, some quantities of interest must be defined, as the objective is to estimate the dangerous areas associated to the accident. Both $CH_4$ and $H_2S$ are flammable, while only $H_2S$ is toxic, therefore it is important to introduce the following quantities:

- LFL: Low Flammability Limit;
- UFL: Upper Flammability Limit;
- IDLH: Immediately Dangerous to Life and Health concentration;
- $LC_{50}$: lethal dose at which 50% of the population is killed in a given exposition time.

The reference values for each species taken from (NIOSH, 1994, OSHA, 2020 and Zlochower et al., 2009) are presented in Table 2.

**Table 2: Flammability and toxicity limits**

| | LFL [mol. conc.] | UFL [mol. conc.] | IDLH [ppm] | $LC_{50}$ [ppm] |
|---|---|---|---|---|
| $CH_4$ | 0.05 | 0.16 | \ | \ |
| $H_2S$ | 0.045 | 0.455 | 100 | 713 |

Since both species of the released mixture are flammable, it is possible to evaluate the LFL and UFL of the mixture using LeChatelier's rule as done in (Liao et al., 2005) remembering that the release mixture has 95% $CH_4$ – 5 % $H_2S$ composition:

$$\mathrm{LFL_{mix}} = \frac{100}{\sum \mathrm{C_i}/\mathrm{LFL_i}} \tag{4}$$

(Analogous for UFL). By Eq. 4 the following values are obtained:

- $LFL_{mix} = 0.049$
- $UFL_{mix} = 0.17$

First of all, to understand the spatial distribution of the pollutant is fundamental to analyze the velocity flow field. From a qualitative point of view, the velocity field obtained at the release height plane is shown in Fig. 6.

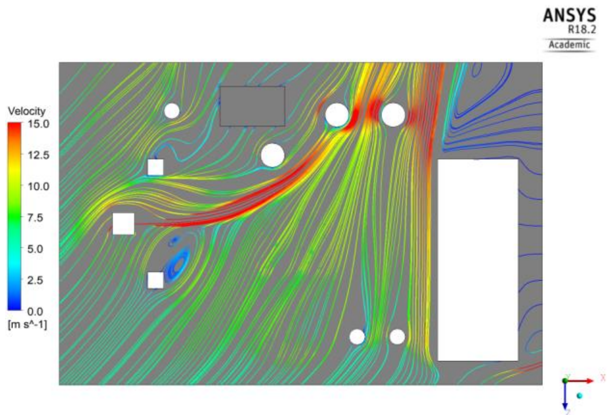


Figure 6: Velocity field in the production deck

The velocity streamlines follow the wind direction near the inlet boundaries b1 and b2, therefore the wind velocity seems to be well reproduced in the deck. The flow becomes quite complex as it interacts with the objects: separation flows appear and secondary vortices are generated. The velocity field analysis is very important because it allows understanding how the pollutants are transported in the domain.

For the purposes of a QRA, it is important to study the flammable and toxic concentration maps. The first one is relevant for people safety and the integrity of the equipment because the ignition of the flammable cloud can lead to a flash fire and a domino effect that involve the equipment integrity. Meanwhile, in the second one, the workers should be subjected to a risk for their health or life.

In Fig. 7 the flammable region, i.e. the region in which the mixture concentration is between $LFL_{mix}$ and $UFL_{mix}$, is shown in red, while in Fig. 8 the toxic regions with $H_2S$ concentration higher than IDLH and $LC_{50}$ are shown respectively in red and yellow on the same section plane of the velocity field.

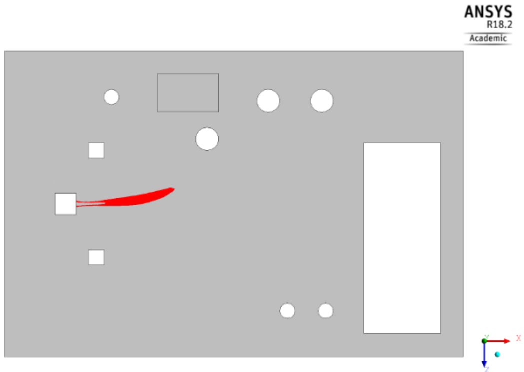


Figure 7: Flammable area

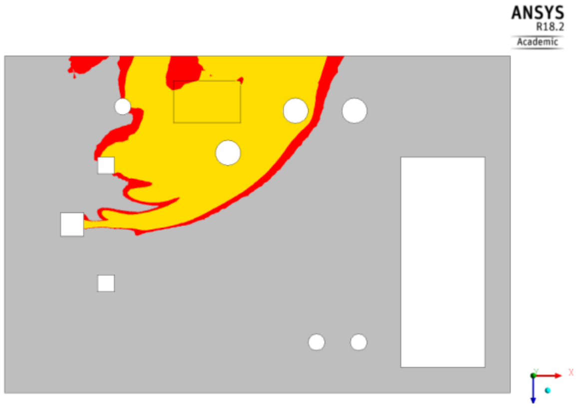


Figure 8: IDHL (red) and $LC_{50}$ (yellow) regions

The flammable area appears as a plume with extension of ~7 m that is slightly deviated by the wind: the velocity of the jet is such that the wind is not affecting too much the plume shape in the first 10 m. The ignition of the mixture can cause an explosion or a fire involving a bigger area of the platform, causing also a possible domino effect depending on the type of components involved in the fire. The toxic area covers a large part of the platform and it is evident that the shape is highly influenced by the wind direction: it can be deduced that the wind condition is a crucial parameter in the assessment of the dangerous areas, and it is the main driver of the pollutant cloud diffusion. It is possible to define the toxic hazardous area and to apply risk control measures for workers. From the comparison of the flammable and toxic areas it can be appreciated that the toxicity is the most dangerous aspect to consider in a release of sour gas to protect the worker health, without considering a possible domino effect due to the flammability. The previous considerations are referred only to a plane section of the platform and it is interesting to see that also the 3D results confirm this trend. In Fig. 9 the flammable cloud is shown, while in Fig. 10 the toxic cloud (IDLH) is shown.

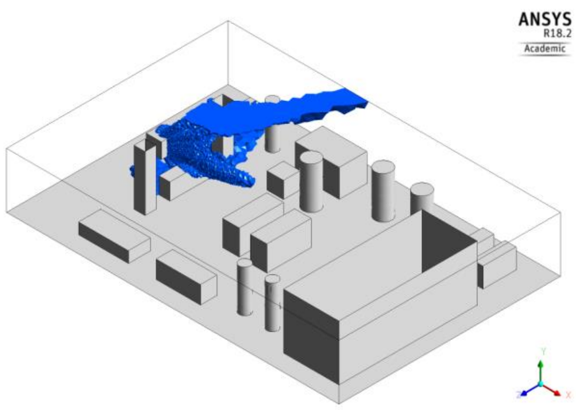


Figure 9: 3D flammable cloud

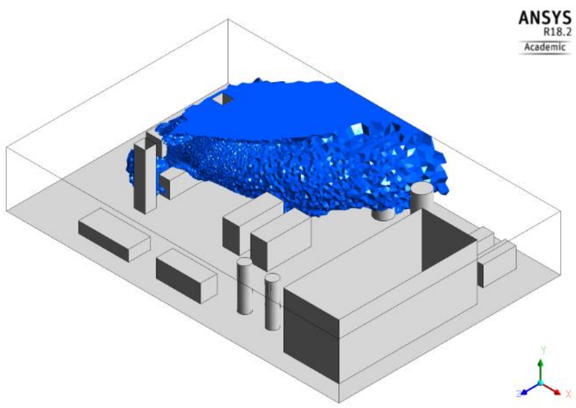


Figure 10: 3D toxic cloud (concentration > IDLH)

The two volumes configurations confirm the considerations made for the 2D results: the toxic cloud involves a larger number of components with respect to the flammable one and it seems to be the most impacting factor on the safety of the system. In addition, the quantities reported in Table 3 give a numerical measure of these differences: it can be noticed that the toxic volume is more than 10 times larger than the flammable one.

**Table 3: mass and volume of flammable and toxic cloud**

| | |
|---|---|
| Flammable cloud volume [$m^3$] | ~26 |
| Flammable cloud mass [kg] | ~29 |
| Toxic cloud volume [$m^3$] | ~328 |
| Toxic cloud mass [kg] | ~369 |

A final important comment must be made about the simulations time of the SB and dispersion. Both simulations are carried out on the same machine that is a Dell Tower 7810 using the same number of cores (8 cores and 64Gb RAM). The SB simulation takes almost 24 h while the dispersion one takes ~3 h. The big difference in the simulation time can be explained considering that, in the dispersion phase, the phenomena to be simulated are very simple and no complex fluid dynamic structure appears. On the other hand, the complexity of the fluid-dynamic structures characterizing the release makes the SB simulation heavier.

## CONCLUSION

In this work, a pressurized sour gas ($CH_4$-$H_2S$ mixture) release simulation is performed using ANSYS Fluent software.
The SBAM approach provides reliable results for a pressurized flammable and toxic gas mixture leakage accidental scenario. Firstly, the physical consistency of the under-expanded jet is analyzed by comparing the CFD results with the corresponding theoretical references. The comparison shows a good accordance between numerical results and theoretical predictions and it is possible to see the presence of the Mach cell and its correct location as predicted by theory. Secondly, it is possible to see that the velocity field in the entire platform is strongly influenced by the presence of the wind and separation flows appear near the obstacles.
The second phase of the proposed approach is the most relevant for the risk assessment procedure; in fact, it allows defining the damage areas of the accidental scenario:

- a flammable area, where the $CH_4$-$H_2S$ mixture is inside the flammable range. In this area, it is fundamental to avoid the interaction between the gas mixture and hot surfaces, flames or sparks to prevent the ignition of the gas cloud and the damage for people and the environment.
- a toxic area, where the $H_2S$ concentration is higher than IDLH. The presence of $H_2S$ means a threat for workers: for this reason, safety equipment needs to be adequate to protect workers from the hazards of $H_2S$.

One of the main outcomes of the work is that the splitting of the phenomenon can reduce dramatically the computational time, since the SB simulation results can be used for several dispersion simulations in which the release position and direction change. In fact, the dispersion simulation time is very low (~3 h) compared to the more complex release one (~24 h). This result can lead to a new approach in QRA, in which several accidental scenarios can be simulated via CFD in a reasonable time.
Finally, a future step deals with the validation. CFD models usually require an experimental validation: for this reason, an experimental campaign is in progress in order to validate the SBAM approach in a novel wind tunnel located in Turin, the SEASTAR wind tunnel, which is presently being calibrated. The experiments using a 1:10 scaled offshore platform mockup can provide significant results for SBAM validation (Moscatello et al., 2020).

## REFERENCES

ANSYS Fluent 18.2, User's Guide, 2018.
CARPIGNANO, A., CORTI, T., UGGENTI, A.C. and GERBONI, R. (2017), "Modelling of a supersonic accidental release in Oil&Gas offshore: Characterisation

of a source box", *GEAM. Geoingengeria ambientale e mineraria*, 58-64.

CASAL, J., (2007), "Evaluation of the effects and consequences of Major Accidents in industrial plants" *Elsevier, Chapter 11.*

CHEN, C.J. and RODI, W., (1980), "Vertical turbulent buoyant jets*", Pergamon Press*.

CHOI, J., HUR, N., KANG, S., LEE, E. D. and LEE, K.B., (2013), "A CFD simulation of hydrogen dispersion for the hydrogen leakage from a fuel cell vehicle in an underground parking garage", *International Journal of Hydrogen Energy*, Vol. 38, Issue 19, 8084-8091.

CRIST, S., GLASS, D. R., and SHERMAN, P. M., (1966), "Study of the highly underexpanded sonic jet", *AIAA Journal*, 68-71.

DAVIDSON, G. (1967), "Simultaneous trajectory and dilution predictions from a simple integral plume model", *Atmospheric Environment*, Vol. 23, 341-349.

DENG, Y., HU, H., YU, B., SUN, D., HOU, L. and LIANG, Y., (2018), "A method for simulating the release of natural gas from the rupture of high-pressure pipelines in any terrain", *Journal of Hazardous Materials*, Vol. 342, 418-428.

DOROUDI, S., POPHALI, A., BUSSMANN, M., TANDRA, D., TRAN, H., (2015), "Modelling Sootblower jet effectiveness with ANSYS Fluent", *Journal of Science & Technology for Forest Products and Processes* Vol. 4, 30-35.

EGGINS, P. L. and JACKSON, D. A., (1974), "Laser-Doppler velocity measurements in an under-expanded free jet", *Journal of Physics D: Applied Physics*, Vol. 7, N. 14.

FRANQUET, E., PERRIER, V., GIBOUT, S. and BRUEL, P. (2015), "Free underexpanded jets in a quiescent medium: A review", *Progress in Aerospace Science*, Vol. 77, 25-53.

IVINGS, M. J., GANT, S. E., SAUNDERS, C. J., and POCOCK, D. J., (2010), "Flammable gas cloud build up in a ventilated enclosure", *Journal of Hazardous Materials*, Vol. 184 (1), 170-176.

LAYFON, D.W., CEDERWALL, R.T., (1987), "Predicting and managing the health risks of sour-gas wells", *JAPCA*, Vol. 37, 1185-1190.

LI, X. J., ZHOU, R. P. and KONOVESSIS, D., (2016). "CFD analysis of natural gas dispersion in engine room space based on multi-factor coupling", *Ocean Engineering*, Vol. 111, 524-532.

LI, D., ZHANG, L., YANG, J. et al., (2014), "Effect of H2S concentration on the corrosion behavior of pipeline steel under the coexistence of H2S and CO2", *Int J Miner Metall Mater*, Vol. 21, 388–394.

LIAO, S., CHENG, Q., JIANG, D. M. and GAO, J., "Experimental study of flammability limits of natural gas-air mixture", *Journal of Hazardous Materials*, Vol. 119, 81-84.

LIU, X., GODBOLE, A., LU, C., MICHAL, G. and VENTON P., (2014), "Source strength and dispersion of CO2 releases from high-pressure pipelines: CFD model using real gas equation of state", *Applied Energy*, Vol. 126, 56-68.

LIU, W., GAO, B., ZHANG, Z., ZHANG, J., ZHANG, D., FAN, M., FU, X., ZHENG, L., LIU, Q., (2010), "$H_2S$ formation and enrichment mechanisms in medium to large scale natural gas fields (reservoirs) in the Sichuan Basin", *Petroleum exploration and development*, Vol. 37, Issue 5.

MI, J., ZHANG, B., SHEN, Z., HUANG, W., CASALINS, A., LIU C., (2017), "The experimental study on H2S generation during thermal recovery process for heavy oil from the Eastern Venezuela Basin", *Journal of Natural Gas Geoscience*, Vol. 2, Issue 3, 201-208.

MOSCATELLO, A., UGGENTI, A.C., IUSO, G., D'AMBROSIO, D., CAFIERO, G., GERBONI, R., CARPIGNANO, A., (2020), "Scaling procedure for designing accidental gas release experiments", *Engineering Computations.*

MUNSON, B., YOUNG, D., OKIISHI, T., HUEBSCH, W., (2009), "Fundamentals of Fluid Mechanics (VI ed.)", *Wiley*.

NECCI, M., TARANTOLA, S., VAMANU, B., KRAUSMANN, E. and PONTE L., (2019), "Lessons learned from offshore oil and gas incidents in the Arctic and other ice-prone seas", *Ocean Engineering* Vol. 185, 12-26.

NIOSH, (1994), "Documentation for Immediately Dangerous to Life or Health Concentration".

NOVEMBRE, N., PODENZANI, F. and COLOMBO, E., (2006), "Numerical study for accidental gas releases from high pressure pipelines", *Proceedings of the European Conference on Computational Fluid Dynamics*.

OSHA, https://www.osha.gov/SLTC/hydrogensulfide/hazards.html#:~:text=The%20explosive%20range%20of%20hydrogen,much%20higher%20than%20the%20PEL. Available at 6/2020.

PATÉ-CORNELL, M., (1993), "Risk analysis and risk management for offshore platforms: Lessons from the Piper Alpha accident", *Journal of Offshore Mechanics and Arctic Engineering*, Vol. 115, 179-190.

VENETSANOS, A.G., BARALDI, D., ADAMS, P., HEGGEM, P.S. and WILKENING, H., (2008), "CFD modelling of hydrogen release, dispersion and combustion for automotive scenarios", *Journal of Loss Prevention in the Process Industries*, Vol. 21, Issue 2, 162-184.

VINNEM, J.E., (2019), "Offshore Risk Assessment vol 2 – Chapter 14 (Fourth Edition)", *Springer*.

VIVALDA, C., GERBONI, R. and CARPIGNANO, A., (2018), "A practical approach to risk-based gas monitoring system design for oil and gas offshore platforms", *Proceedings of the 14th Probabilistic Safety Assessment and Management Conference*.

WARNER, J.L., BASKIN, D.K., HWANG, R.J., CARLSON, R.M., and CLARK, M.E., (2007), "Geochemical Evidence for Two Stages of Hydrocarbon Emplacement and the Origin of Solid Bitumen in the Giant Tengiz Field, Kazakhstan", *Oil and Gas of the Greater Caspian Area*, Pinar O. Yilmaz, Gary H. Isaksen.

WORDEN R.H., SMALLEY, P.C., BARCLAY, S.A, 2003, "$H_2S$ and diagenetic pyrite in North Sea sandstones: due to TSR or organic sulphur compound cracking?", *Journal of Geochemical Exploration*, Vol. 78 79, 487-491.

ZAMEJC, E. (2014), "API Standard 521 new alternative method to evaluate fire relief for pressure relief device sizing and depressuring system design", *Journal of Loss Prevention in the Process Industries,* Vol. 27, 21-31.

ZEMPOLICH, W., NEGRI, A., LEO, C., VAN OJIK, K. and VERDEL, A., (2002), "Kashagan Discovery: An Example of the Successful Use of a Multi-disciplined Approach in Reducing Geologic Risk", *AAPG Annual Meeting,* March 10-13, 2002 Houston, Texas.

ZLOCHOWER, I. and GREEN, G., "The limiting oxygen concentration and flammability limits of gases and gas mixtures", *Journal of Loss Prevention in the Process Industries*, Vol. 22, 499-505.